Available online at www.sciencedirect.com

SCIENCE DIRECT®

ELSEVIER

International Journal of Solids and Structures 41 (2004) 6949–6962

INTERNATIONAL JOURNAL OF SOLIDS and STRUCTURES

www.elsevier.com/locate/ijsolstr

Analytical solution of two intersecting cylindrical shells subjected to transverse moment on nozzle

M.D. Xue *, D.F. Li *, K.C. Hwang

Department of Engineering Mechanics, Institute of Solid Mechanics, Tsinghua University, Beijing 100084, PR China

Received 4 December 2003; received in revised form 24 May 2004
Available online 20 July 2004

Abstract

In this paper a theoretical solution for two normally intersecting cylindrical shells subjected to transverse moment on the branch pipe is presented, which based on thin shell theory. The accurate shell equations, boundary conditions and calculating methods are adopted so that the solution presented can be applicable up to $d/D \leqslant 0.8$ and $\lambda = d/(DT)^{1/2} \leqslant 8$. The presented results are in very good agreement with experimental and numerical results for ORNL-1 Model. They are also in agreement with the results obtained by WRC Bulletin 297 when d/D is small.

Keywords: Cylindrical shell; Thin shell theory; Tee-joint; Stress analysis; Pressure vessel

1. Introduction

Two intersecting cylindrical shells subjected to internal pressure and external moments are of common occurrence in pressure vessel and piping industry. The highest stress intensity often occurs in the vicinity of junction, which is a complicated space curve when the diameter ratio, d/D, of the branch pipe relative to the main shell increases. This topic has attracted many researchers' attention due to its importance since 1960s (see Reidelbach, 1961; Eringen et al., 1965, 1969; Eringen and Suhubi, 1965; Van Dyke, 1965, 1967; Qian et al., 1965; Yamamoto et al., 1969; Hansberry and Jones, 1969; Lekerkerker, 1972; Steele and Steele, 1983). In order to evaluate the significant local stresses in cylindrical shells due to external moments on branch pipes, a thin shell theoretical solution were presented by Bijlaard (1954, 1955a,b). The mathematical model adopted by Bijlaard is a cylindrical shell without branch pipe subjected to a local loading (force or moment) in a square region and his solutions are applied by Wichman et al. (1965) to WRC Bulletin No. 107, which is used by design analysts since 1965. Steele and Steele (1983) and Khathlan (1986) presented an approximate analytical solution of two normally intersecting cylindrical shells based on shallow shell theory. The design method and tabular data obtained by Steele's program FAST2 were presented for designers in WRC

* Corresponding authors. Tel.: +86-10-62772902; fax: +86-10-62771824.
E-mail addresses: xuemd@mail.tsinghua.edu.cn (M.D. Xue), lidongfeng95@tsinghua.org.cn (D.F. Li).

0020-7683/$ - see front matter
doi:10.1016/j.ijsolstr.2004.05.057

Bulletin No. 297 by Mershon et al. (1984) as a supplement to WRC Bulletin No. 107. WRC Bulletin 297 provides data for the diameter ratio $\rho_0 = d/D$ up to approximately 0.5 and includes the effects of nozzle thickness. Moffat (1985), Moffat et al. (1991) obtained numerical solutions and developed design methods based on 3-D FEM and experimental results. The limitations of application of the design method in BS 806 are $5 \leqslant D/T \leqslant 70$ and $d/D \leqslant t/T \leqslant 1$, where t and T denote the thicknesses of nozzle and cylinder, respectively. Although researchers and designers have expanded the great efforts to overcome the significant difficulties on mathematics and analysis method, the design procedures for branch junctions are still in need of improvement.

The authors of the present paper, Xue et al. (1991, 1995a,b, 1996, 1999, 2000) and Deng et al. (1991) developed a thin shell theoretical method for two orthogonally intersecting cylindrical shells with large d/D ratio. The intersecting shells subjected to internal pressure and run pipe moments were investigated by Xue et al. (1995b, 1996) and Xue et al. (1999, 2000), respectively. Comparing with analytical solutions by previous researchers, the four aspects in the present theoretical solution are improved as follows: (1) the modified Morley's equation, which is applicable to the cases $\lambda = d/(DT)^{1/2} \gg 1$ with the accuracy order $O(T/R)$, is adopted instead of Donnell's shallow shell equation; (2) five coordinate systems in three spaces (two-dimensional cylindrical surfaces of main shell and branch pipe and three-dimensional space) and the accurate expressions of the intersecting curve are used instead of approximate expressions, which bring about significant error when $d/D > 0.3$; (3) the accurate continuity conditions for forces, moments, displacements and rotations at the intersection curve of the two cylinders are adopted instead of approximate continuity conditions; (4) the great mathematical difficulties coursed by the accurate but very complicated formulations are overcome. As a new progress of theoretical solution and design criteria research developed by the authors, the stress analysis based on the theory of thin shell is carried out for cylindrical shells with normally intersecting nozzles subjected to external branch pipe moments.

2. Mathematical model

Two intersecting cylindrical shells subjected to external branch pipe moments, i.e., out-of plane moment M_{xb}, in-plane moment M_{yb} and torsion moment M_{zb}, and five coordinate systems, i.e., main coordinate system, (ξ, φ), and polar coordinates, (α, β), on developed cylindrical shell surface, (θ, ς) on nozzle surface, global Cartesian coordinates (x, y, z) and circular cylindrical coordinates (ρ, θ, z) in 3-D space, adopted in this paper are shown in Fig. 1, where Γ denote the intersecting curve. The cantilever main shell is supported at one end with the following boundary conditions:

$$T_\xi = 0,\ \ u_\varphi = 0,\ \ u_n = 0,\ \ M_\xi = 0 \quad \text{at } x = -L\ (L \gg R) \tag{1}$$

Each of the three load cases can be considered as the superposition of some basic categories symmetrical or antisymmetrical about $\theta = 0$ and $\theta = \pi/2$. As an example, the loading case of out-of plane moment M_{xb}, which causes the most serious stress concentration, can be considered as the superposition of the following two categories. That is, category (a): main cylindrical shell with branch pipe simple supported at the two ends and subjected to out-plane branch pipe moment M_{xb} as shown in Fig. 2(a), which is antisymmetric about $\theta = 0$ and symmetric about $\theta = \pi/2$; and category (b): main shell subjected to torsion moments, $M_{xb}/2$, at the two ends as shown in Fig. 2(b), which is antisymmetric about both $\theta = 0$ and $\theta = \pi/2$. Because the solution of category (b) has been given by Xue et al. (1999, 2000), in the present paper, we pay our attention to solve the category (a), i.e., simple supported main shell subjected to branch moment.

The thin shell theoretical solution for the main shell with cutout, Γ, on which moment M_{xb} is applied, is obtained by superposing the particular solution on the homogeneous solution. The double Fourier series solution of Timoshenko's equations (1959) in the coordinates (ξ, ϕ) is taken as a particular solution and the

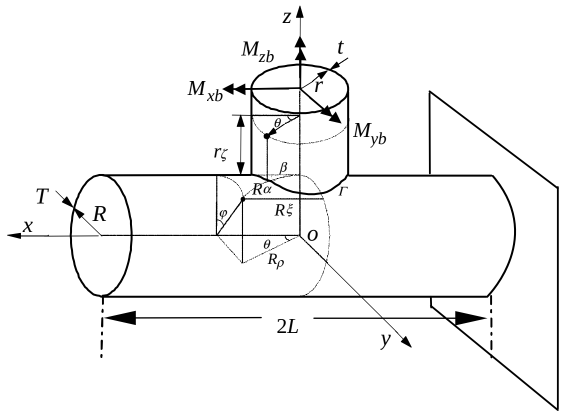

Fig. 1. Calculated model and five coordinate systems.

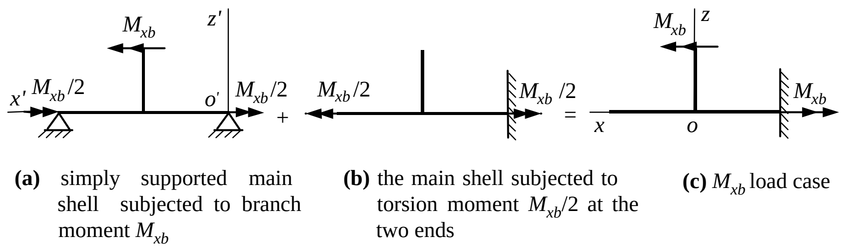

Fig. 2. Superposing two basic categories into M_{xb} load case: (a) simply supported main shell subjected to branch moment M_{xb}; (b) the main shell subjected to torsion moment $M_{xb}/2$ at the two ends; (c) M_{xb} load case.

Xue et al.'s solution (1999, 2000) in the polar coordinates (α, β), as the homogeneous solution based on the modified Morley (1959) equation shown in Xue et al. (2000) instead of the Donnell shallow shell equation. The displacement function solution for the nozzle with a nonplanar boundary curve, Γ, is obtained on the basis of the Goldenveizer equation (1961) in the coordinates (θ, ζ) instead of Timoshenko equation. The boundary general forces and displacements of both main shell and branch pipe at the intersecting curve, Γ, are all transformed into global coordinate system, (ρ, θ, z), and expanded in Fourier series of θ. Then the unknown constants in general solutions of both main shell and branch pipe could be solved by the continuity conditions of general forces and displacements.

3. The theoretical solution of cylindrical shell with cut-out subjected to out-of plane branch pipe moment

The general solution of this problem is divided into the following two parts: (1) a particular solution, which is in equilibrium with M_{xb} but does not satisfy the boundary conditions at the cut-out; (2) general solution of the homogeneous equation of cylindrical shell. The sum of the two parts with some integral constants becomes the general solution of this problem and the unknown constants could be determined by the boundary conditions at the edge of the cut-out.

3.1. A particular solution in equilibrium with M_{xb}

A thin shell theoretical solution for a simply supported cylindrical shell subjected to a vertical force system q_z distributed over a central square region in the developed surface (ξ, φ), defined by $|\xi| \leqslant c/R$, $|\varphi| \leqslant c/R$, is taken as a particular solution of the problem. The vertical force system in the region, q_z, is distributed linearly in φ direction and uniformly in ξ, as shown in Fig. 3. The vertical force system, q_z, is statically equivalent to M_{xb}. [1]

The Timoshenko equations in coordinates (ξ, φ) for cylindrical shell subjected to arbitrary distributed load is adopted as follows:

$$\left(\frac{\partial^2}{\partial\xi^2} + \frac{1-v}{2}\frac{\partial^2}{\partial\varphi^2}\right)u_\xi + \frac{1+v}{2}\frac{\partial^2 u_\varphi}{\partial\xi\partial\varphi} + v\frac{\partial u_n}{\partial\xi} = -\frac{R^2(1-v^2)}{ET}q_\xi \tag{2a}$$

$$\frac{1+v}{2}\frac{\partial^2 u_\xi}{\partial\xi\partial\varphi} + \left[\frac{1-v}{2}\frac{\partial^2}{\partial\xi^2} + \frac{\partial^2}{\partial\varphi^2}\right]u_\varphi + \frac{\partial}{\partial\varphi}(1 - a^2\nabla^2)u_n = -\frac{R^2(1-v^2)}{ET}q_\varphi \tag{2b}$$

$$v\frac{\partial u_\xi}{\partial\xi} + \frac{\partial}{\partial\varphi}\left[1 - a^2\left((2-v)\frac{\partial^2}{\partial\xi^2} + \frac{\partial^2}{\partial\varphi^2}\right)\right]u_\varphi + (1 + a^2\nabla^2\nabla^2)u_n = \frac{R^2(1-v^2)}{ET}q_n \tag{2c}$$

where $\xi = x/R$, $a^2 = T^2/(12R^2)$, $\nabla^2 = \frac{\partial^2}{\partial\varphi^2} + \frac{\partial^2}{\partial\xi^2}$, E is Young's modulus, v is Poisson's ratio, q_ξ, q_φ and q_n are the distributed loads applied on the shell.

In view of the deformation field symmetric with respect to the plane $\xi = 0$ and antisymmetric with respect to the plane $\varphi = 0, \pi$, Eqs. (2a–c) with simple supported boundary conditions at $\xi = \pm L/R$ can be solved by expanding the displacements and external load in double infinite Fourier series as follows:

$$q_\xi = 0, \quad q_\varphi = -\sum_{m=0}^{\infty}\sum_{n=1}^{\infty} q_{mn}^{(2)}\cos(m\varphi)\sin(\lambda_n\xi'), \quad q_n = \sum_{m=1}^{\infty}\sum_{n=1}^{\infty} q_{mn}^{(3)}\sin(m\varphi)\sin(\lambda_n\xi') \tag{3a,b,c}$$

$$u_\xi = \sum_{m=1}^{\infty}\sum_{n=1}^{\infty} U_{mn}\sin(m\varphi)\cos(\lambda_n\xi'), \quad u_\varphi = -\sum_{m=0}^{\infty}\sum_{n=1}^{\infty} V_{mn}\cos(m\varphi)\sin(\lambda_n\xi') \tag{4a,b}$$

$$u_n = \sum_{m=1}^{\infty}\sum_{n=1}^{\infty} W_{mn}\sin(m\varphi)\sin(\lambda_n\xi') \tag{4c}$$

where $\lambda_n = \frac{(2n-1)\pi R}{2L}$; $n = 1, 2, \ldots$; $\xi' = (x+L)/R$.

The vertical force system and its radial and tangential components are:

$$q_z(\xi,\varphi) = \begin{cases} q\frac{\sqrt{2}\varphi}{\rho_0}, & |\xi| \leqslant \rho_0/\sqrt{2}, |\varphi| \leqslant \rho_0/\sqrt{2} \\ 0, & |\xi| > \rho_0/\sqrt{2} \text{ or } |\varphi| > \rho_0/\sqrt{2} \end{cases}, \quad q_\varphi = -q_z\sin\varphi \tag{5}$$
$$q_n = q_z\cos\varphi$$

where $\rho_0 = r/R$, from the equivalence of q_z-system to M_{xb},

[1] Reference to Bijlaard (1955b) a simply supported cylindrical shell is subjected to distributed linearly radial force system, q_n, whose resultants include not only moment, M_{xb}, but also force, F_y. Therefore, in order to raise accuracy of the solutions in the present paper the shell is subjected to vertical force system, q_z, instead of radial force system, q_n, because the latter may cause a significant error when the diameter ratio d/D is not small.

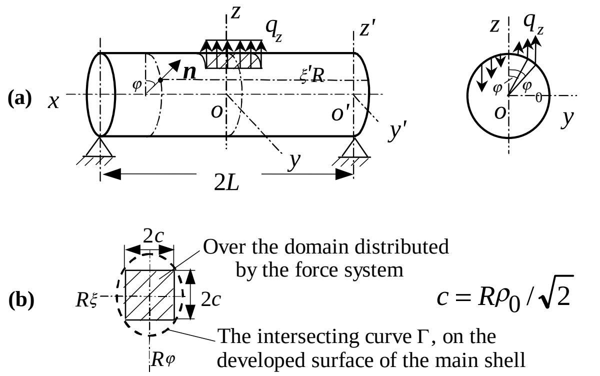

Fig. 3. The analytic model of particular solution: (a) the distributed force system q_z equivalent to M_{xb}; (b) the domain distributed by force system q_z.

$$q = \frac{M_{xb}}{4R^3} \Big/ \left(\sin\frac{\rho_0}{\sqrt{2}} - \frac{\rho_0}{\sqrt{2}}\cos\frac{\rho_0}{\sqrt{2}} \right) \tag{6}$$

Then the coefficients in Fourier series Eq. (3b,c) are

$$q_{mn}^{(2)} = \begin{cases} -\dfrac{2\sqrt{2}}{\pi}\dfrac{qR}{\rho_0 L}\displaystyle\int_0^{\rho_0/\sqrt{2}}\int_0^{\rho_0/\sqrt{2}} (\varphi\sin\varphi\sin\lambda_n\xi)\,\mathrm{d}\xi\,\mathrm{d}\varphi, & m = 0 \\ -\dfrac{4\sqrt{2}}{\pi}\dfrac{qR}{\rho_0 L}\displaystyle\int_0^{\rho_0/\sqrt{2}}\int_0^{\rho_0/\sqrt{2}} (\varphi\sin\varphi\cos m\varphi\sin\lambda_n\xi)\,\mathrm{d}\xi\,\mathrm{d}\varphi, & m \geqslant 1 \end{cases} \tag{7a}$$

$$q_{mn}^{(3)} = \frac{4\sqrt{2}qR}{\pi\rho_0 L}\int_0^{\rho_0/\sqrt{2}}\int_0^{\rho_0/\sqrt{2}} (\varphi\cos\varphi\sin m\varphi\sin\lambda_n\xi)\,\mathrm{d}\xi\,\mathrm{d}\varphi, \quad m \geqslant 1 \tag{7b}$$

Substituting Eqs. (3) and (4) into (2a–c), the coefficients in Fourier series (4a–c) can be solved from the following system of linear algebraic equations:

$$-\left(\lambda_n^2 + \frac{1-v}{2}m^2\right)U_{mn} + \left(\frac{1+v}{2}\lambda_n m\right)V_{mn} + v\lambda_n W_{mn} = 0 \tag{8a}$$

$$\left(-\frac{1+v}{2}\lambda_n m\right)U_{mn} + \left(-\frac{1-v}{2}\lambda_n^2 - m^2\right)V_{mn} + m[1 + a^2(\lambda_n^2 + m^2)]W_{mn} = -\frac{R^2(1-v^2)}{ET}q_{mn}^{(2)} \tag{8b}$$

$$-v\lambda_n U_{mn} + m[1 + a^2((2-v)\lambda_n^2 + m^2)]V_{mn} + [1 + a^2(m^4 + 2\lambda_n^2 m^2 + \lambda_n^4)]W_{mn} = \frac{R^2(1-v^2)}{ET}q_{mn}^{(3)} \tag{8c}$$

The particular solution for resultant forces and moments could be obtained from displacements by means of geometric and elastic relations (see Timoshenko and Woinowsky-Krieger, 1959). The general displacements and forces at the closed curve, Γ, can be expressed by substituting the values of ξ_Γ, φ_Γ:

$$\xi = \xi_\Gamma = \rho_0\cos\theta, \quad \varphi = \varphi_\Gamma = \sin^{-1}(\rho_0\sin\theta) \tag{9a,b}$$

into Eqs. (4a–c) and related expressions of forces and moments. Therefore, they are in equilibrium with M_{xb}, satisfied for all the basic equations and the boundary conditions at the two simple supported ends of cylindrical shell, so that could be regarded as a particular solution of the boundary forces and displacements at the cutout of the mean shell.

3.2. The homogeneous solution of cylindrical shells with cut-out

The general solution of homogeneous partial differential equation for a cylindrical shell subjected to any boundary conditions but no external load acting on the surface can be obtained by solving the modified Morley's equation by Zhang et al. (1991):

$$\left(\nabla^2+\frac{1}{2}+2\mu\sqrt{\mathrm{i}}\frac{\partial}{\partial\xi}\right)\left(\nabla^2+\frac{1}{2}-2\mu\sqrt{\mathrm{i}}\frac{\partial}{\partial\xi}\right)\chi=0 \tag{10}$$

Unlike Donnell's shallow shell equation, Eq. (10) has the same order of accuracy as the theory of thin shell and is applicable up to $r/\sqrt{RT}\gg 1$ (see Xue et al., 1991). Here,

$$\chi=u_n+\mathrm{i}\frac{4\mu^2}{ETR}\phi \tag{11}$$

where u_n denotes the normal displacement; ϕ is Airy's stress function and

$$4\mu^2=[12(1-v^2)]^{1/2}R/T,\quad \nabla^2=\frac{\partial^2}{\partial\xi^2}+\frac{\partial^2}{\partial\varphi^2}=\frac{\partial^2}{\partial\alpha^2}+\frac{\partial}{\alpha\,\partial\alpha}+\frac{\partial^2}{\alpha^2\,\partial\beta^2} \tag{12}$$

Considering symmetry with respect to $\beta=0$ and the antisymmetry with respect to $\beta=\pi/2$, the solution of Eq. (12) is as follows:

$$\chi=\sum_{k=0}^{\infty}\sum_{n=1}^{\infty}C_nF_{kn}(\alpha)\sin(m\beta),\quad (m=2k+1) \tag{13}$$

where

$$F_{kn}=(-1)^k\left(1-\frac{1}{2}\delta_{m0}\right)[J_{m-n}(\sqrt{-\mathrm{i}}\mu\alpha)+J_{-m-n}(\sqrt{-\mathrm{i}}\mu\alpha)]H_n(\eta\alpha),\quad (k=0,1\ldots;\ n=1,2\ldots) \tag{14}$$

$$C_n=C_{n1}+\mathrm{i}C_{n2},\quad \delta_{mn}=\begin{cases}0, & m\neq n\\ 1, & m=n\end{cases}\qquad (k=0,1\ldots;\ n=1,2\ldots) \tag{15a,b}$$

In Eq. (14) J_n and H_n are nth order Bessel and Hankel functions, respectively and

$$\eta=\left(\frac{1}{2}-\mathrm{i}\mu^2\right)^{1/2} \tag{16}$$

The components of forces, moments, displacements and rotations in the main shell are all expressed through the partial derivatives of χ with respect to α and β, $\chi^{(i,j)}=\frac{\partial^{(i+j)}\chi}{\partial\alpha^i\partial\beta^j}$, as shown by Xue et al. (1995a,b). For example, u_α and u_β can be expanded in Fourier series as follows:

$$u_\alpha=\sum_{k=0}^{\infty}U_k(\alpha)\sin m\beta,\quad u_\beta=-\sum_{k=0}^{\infty}V_k(\alpha)\cos m\beta \tag{17a,b}$$

where

$$U_k=\alpha R\left(f_k-\alpha\frac{\mathrm{d}g_k}{\mathrm{d}\alpha}+mh_k\right)\Big/(1-m^2),\quad V_k=(\alpha Rg_k-U_k)/m\qquad (m=2k+1,\ k=1,2\ldots) \tag{18a,b}$$

$$U_0=\int_{\rho_0}^{\alpha}Rf_0(t)\,\mathrm{d}t+u_{\varphi0},\quad V_0=(\alpha Rg_0-U_0) \tag{19a,b}$$

In Eqs. (18) and (19) the functions f_0, g_0, f_k, g_k and h_k can be expressed in terms of χ and $\chi^{(i,j)}$, as shown in Xue et al. (1999) and Eqs. (19a,b) are different from Eq. (22b) in Xue et al. (1999), where, $u_{\varphi 0}$ is a rigid body displacement and supposed to be zero.

The boundary forces and displacements at the hole edge, Γ, are obtained by substituting the values of α_Γ, β_Γ:

$$\alpha_\Gamma = \sqrt{\rho_0^2 \cos^2\theta + (\sin^{-1}(\rho_0 \sin\theta))^2}, \quad \beta_\Gamma = \sin^{-1}[\sin^{-1}(\rho_0 \sin\theta)/\alpha_\Gamma] \tag{20a,b}$$

into Eqs. (17a,b), the real part of χ in Eq. (13), the expressions of rotation, γ_v and Kirchhoff general forces, T_v, S_v, Q_v, M_v (see Xue et al., 1991, 1995b, 1999).

3.3. Boundary forces and displacements at the cut out in main shell

Superposing the particular solution, which is in equilibrium with M_{xb} and given in Section 3.1, on the homogeneous solution in Section 3.2 the general solution can be obtained, which satisfies all the basic equations of cylindrical shell and any prescribed boundary conditions. The boundary general displacement and force vectors, $\boldsymbol{F}$ and $\boldsymbol{u}$, at Γ can be decomposed in global coordinates (ρ, θ, z) as follows:

$$\boldsymbol{F} = T_v \boldsymbol{i}_v + S_v \boldsymbol{i}_t - Q_v \boldsymbol{i}_n = F_\rho \boldsymbol{i}_\rho + F_\theta \boldsymbol{i}_\theta + F_z \boldsymbol{i}_z \tag{21a}$$

$$\boldsymbol{u} = u_\alpha \boldsymbol{i}_\alpha + u_\beta \boldsymbol{i}_\beta + u_n \boldsymbol{i}_n = u_\rho \boldsymbol{i}_\rho + u_\theta \boldsymbol{i}_\theta + u_z \boldsymbol{i}_z \tag{21b}$$

They are periodic functions of θ with parameter ρ_0 occurring in Eqs. (9a,b) and (20a,b), so can be expanded in Fourier series of θ and truncated after the items with either $k = K (m = 2K + 1)$ or $n = 2K + 1$:

$$F_\rho = \sum_{k=0}^{K} \sum_{n=1}^{2K+1} \sum_{i=1}^{2} (C_{ni} f_{kni}^\rho + \hat{f}_k^\rho) \sin m\theta, \quad F_\theta = -\sum_{k=0}^{K} \sum_{n=1}^{2K+1} \sum_{i=1}^{2} (C_{ni} f_{kni}^\theta + \hat{f}_k^\theta) \cos m\theta \tag{22a,b}$$

$$F_z = \sum_{k=0}^{K} \sum_{n=1}^{2K+1} \sum_{i=1}^{2} (C_{ni} f_{kni}^z + \hat{f}_k^z) \sin m\theta, \quad M_v = \sum_{k=0}^{K} \sum_{n=1}^{2K+1} \sum_{i=1}^{2} (C_{ni} f_{kni}^m + \hat{f}_k^m) \sin m\theta \tag{22c,d}$$

$$u_\rho = \sum_{k=0}^{K} \sum_{n=1}^{2K+1} \sum_{i=1}^{2} (C_{ni} u_{kni}^\rho + \hat{u}_k^\rho) \sin m\theta, \quad u_\theta = -\sum_{k=0}^{K} \sum_{n=1}^{2K+1} \sum_{i=1}^{2} (C_{ni} u_{kni}^\theta + \hat{u}_k^\theta) \cos m\theta \tag{23a,b}$$

$$u_z = \sum_{k=0}^{K} \sum_{n=1}^{2K+1} \sum_{i=1}^{2} (C_{ni} u_{kni}^z + \hat{u}_k^z) \sin m\theta, \quad \gamma_v = \sum_{k=0}^{K} \sum_{n=1}^{2K+1} \sum_{i=1}^{2} (C_{ni} u_{kni}^m + \hat{u}_k^m) \sin m\theta \tag{23c,d}$$

where the first items come from homogeneous solution with $4K + 2$ unknowns C_{ni}, and the second, from particular solution. The Fourier coefficients $f_{kni}^\rho, f_{kni}^\theta \ldots, u_{kni}^\rho \ldots, u_{kni}^m$ and $\hat{f}_k^\rho, \hat{f}_k^\theta \ldots, \hat{u}_k^\rho \ldots, \hat{u}_k^m$ are definite integral expressions, which involve complicated and several oscillatory integrands, and are calculated by Filon numerical integration (see Davis and Rabinowitz, 1984) instead of Gauss integration in order to overcome numerical difficulty.

4. The solution for a semi-infinite long pipe with a nonplanar end subjected to a moment M_{xb}

The branch pipe of a tee-joint is considered as a semi-infinite long cylindrical shell with a curved boundary Γ. The general solution of the pipe subjected to a moment M_{xb} consists of a particular solution and homogeneous solution. The following membrane theoretical solution can be adopted as a particular solution:

$$\hat{T}_\varsigma = \frac{M_{xb}}{\pi r^2}\sin\theta, \quad \hat{T}_{\varsigma\theta} = \hat{T}_\theta = \hat{M}_\varsigma = \hat{M}_\theta = \hat{M}_{\varsigma\theta} = 0 \tag{24a,b}$$

$$\hat{u}_\theta = -\frac{M_{xb}}{2Et\pi r}\varsigma^2\cos\theta, \quad \hat{u}_\varsigma = \frac{M_{xb}}{Et\pi r}\varsigma\sin\theta, \quad \hat{u}_\rho = -\frac{M_{xb}}{Et\pi r}\left(v + \frac{\varsigma^2}{2}\right)\sin\theta \tag{25a,b,c}$$

$$\hat{\gamma}_\theta = -\frac{vM_{xb}}{Et\pi r}\cos\theta, \quad \hat{\gamma}_\varsigma = -\frac{M_{xb}}{Et\pi r}\varsigma\sin\theta \tag{25d,e}$$

The homogeneous solution are obtained by solving Goldenveizer equation in the coordinates (θ, ζ) (see Goldenveizer, 1961) as follows:

$$\nabla^8\psi + 4\lambda_t^4\frac{\partial^4\psi}{\partial\varsigma^4} + (8 - 2v^2)\frac{\partial^6\psi}{\partial\zeta^4\partial\theta^2} + 8\frac{\partial^6\psi}{\partial\zeta^2\partial\theta^4} + 2\frac{\partial^6\psi}{\partial\theta^6} + 4\frac{\partial^4\psi}{\partial\zeta^2\partial\theta^2} + \frac{\partial^4\psi}{\partial\theta^4} = 0 \tag{26}$$

where ψ is displacement function. The components of displacement are expressed through the partial derivatives of ψ as shown in Goldenveizer (1961). For closed shell ψ is a periodic function of θ and can be expanded in Fourier series as follows:

$$\psi = \sum_{k=0}^{\infty}\sum_{l=1}^{8} D_{kl}g_{kl}(\varsigma)\sin m\theta \quad (m = 2k+1,\ \ k = 0, 1, 2\ldots) \tag{27}$$

where

$$\nabla^2 = \frac{\partial^2}{\partial\theta^2} + \frac{\partial^2}{\partial\varsigma^2}, \quad \lambda_t = [3(1 - v^2)r^2/t^2]^{1/4} \tag{28a,b}$$

Substituting Eq. (27) into Eq. (26), we get the ordinary differential equation for $g_{kl}(\zeta)$:

$$\frac{\mathrm{d}^8 g}{\mathrm{d}\varsigma^8} - 4m^2\frac{\mathrm{d}^6 g}{\mathrm{d}\varsigma^6} + [6m^4 - 2m^2(4 - v^2) + 4\lambda_t^4]\frac{\mathrm{d}^4 g}{\mathrm{d}\varsigma^4} - 4m^2(m^2 - 1)^2\frac{\mathrm{d}^2 g}{\mathrm{d}\varsigma^2} + m^4(m^2 - 1)^2 g = 0 \tag{29}$$

Instead of the approximate method given by Goldenveizer (1961), an exact solution is adopted in order to improve the accuracy for $m \neq 1$ but m not necessarily large. The characteristic equation of Eq. (29) is

$$\begin{aligned} &S^8 - 4m^2S^6 + [6m^4 - 2m^2(4 - v^2) + 4\lambda_t^4]S^4 - 4m^2(m^2 - 1)^2S^2 + m^4(m^2 - 1)^2 = 0 \\ &\quad (m = 2k+1,\ \ k = 0, 1, 2\ldots) \end{aligned} \tag{30a}$$

When $m = 1$, considering $2(1 - v^2) \ll 4\lambda_t^4$ Eq. (30a) is turned into

$$S^8 - 4S^6 + 4\lambda_t^4 S^4 = 0 \tag{30b}$$

Eq. (30) is a quartic algebraic equation with real coefficients for s^2 and so generally has double conjugate roots. Therefore, the roots of Eq. (30a) should be expressed as follows:

$$S_{1,2,5,6} = \mp a_{m1} \mp \mathrm{i}b_{m1}, \quad S_{3,4,7,8} = \mp a_{m2} \mp \mathrm{i}b_{m2} \tag{31}$$

where the method of solving a_{m1}, b_{m1}, a_{m2} and b_{m2} is referred to Wang and Guo (2000). Specially, when $m = 1$: a_{m1}, $b_{m1} = 0$, $a_{m2} = (\lambda_t^2 + 1)^{1/2}$, $b_{m2} = (\lambda_t^2 - 1)^{1/2}$. Due to the boundary conditions when $\varsigma \to \infty$, the four items of the solutions of the eighth order partial differential equation (26) vanish, so that only $4k$ functions $g_{kl}(\varsigma)$ $(l = 1, 2, 3, 4)$ remain in the Fourier series (27) as follows:

$$g_{m1}(\varsigma) = \begin{cases} 1, & m = 1 \\ e^{-a_{m1}\varsigma}\sin(b_{m1}\varsigma), & m > 1 \end{cases}, \quad g_{m2}(\varsigma) = \begin{cases} \varsigma, & m = 1 \\ e^{-a_{m1}\varsigma}\cos(b_{m1}\varsigma), & m > 1 \end{cases} \tag{32a,b}$$

$$g_{m3}(\varsigma) = \begin{cases} e^{-\varsigma\sqrt{\lambda_t^2+1}}\sin\left(\varsigma\sqrt{\lambda_t^2-1}\right), & m = 1 \\ e^{-a_{m2}\varsigma}\sin(b_{m2}\varsigma), & m > 1 \end{cases},$$
$$g_{m4}(\varsigma) = \begin{cases} e^{-\varsigma\sqrt{\lambda_t^2+1}}\cos\left(\varsigma\sqrt{\lambda_t^2-1}\right), & m = 1 \\ e^{-a_{m2}\varsigma}\cos(b_{m2}\varsigma), & m > 1 \end{cases} \tag{32c,d}$$

The homogeneous solutions of boundary displacements, rotations, forces and moments at the intersecting curve, Γ, are expressed in terms of $\psi^{(i,j)}(\zeta_\Gamma, \theta)$ (see Xue et al., 1999, 2000) where $\zeta_\Gamma(\theta)$ is the expression for Γ in coordinates (ς, θ):

$$\varsigma_\Gamma = (1 - \rho_0^2 \sin^2\theta)^{1/2}/\rho_0 = \varsigma_\Gamma(\rho_0, \theta) \tag{33}$$

Superposing the homogeneous solution, truncated after the items $k = K$, on a particular solution given in Eqs. (24) and (25), and substituting Eq. (33), the boundary displacement vector, $\boldsymbol{u}^{(t)} = u_v^{(t)}\boldsymbol{i}_v + u_t^{(t)}\boldsymbol{i}_t + u_n^{(t)}\boldsymbol{i}_n = u_\rho^{(t)}\boldsymbol{i}_\rho + u_\theta^{(t)}\boldsymbol{i}_\theta + u_z^{(t)}\boldsymbol{i}_z$ and force vector, $\boldsymbol{F}^{(t)} = F_v^{(t)}\boldsymbol{i}_v + F_t^{(t)}\boldsymbol{i}_t + F_n^{(t)}\boldsymbol{i}_n = F_\rho^{(t)}\boldsymbol{i}_\rho + F_\theta^{(t)}\boldsymbol{i}_\theta + F_z^{(t)}\boldsymbol{i}_z$, rotation $\gamma_v^{(t)}$ and moment $M_v^{(t)}$ are obtained. Obviously, they are all periodic functions of θ with the parameter ρ_0 and $(4K+4)$ unknowns D_{kl} $(m = 2k+1, k = 0, 1, 2\ldots, l = 1, 2, 3, 4)$, and can be re-expanded in Fourier series of θ as follows:

$$F_\rho^{(t)} = \sum_{k=0}^{K}\sum_{j=0}^{K}\sum_{l=1}^{4}\left(D_{jl}f_{kjl}^{(t)\rho} + \hat{f}_k^{(t)\rho}\right)\sin m\theta, \quad F_\theta^{(t)} = -\sum_{k=0}^{K}\sum_{j=0}^{K}\sum_{l=1}^{4}\left(D_{jl}f_{kjl}^{(t)\theta} + \hat{f}_k^{(t)\theta}\right)\cos m\theta \tag{34a,b}$$

$$F_z^{(t)} = \sum_{k=0}^{K}\sum_{j=0}^{K}\sum_{l=1}^{4}\left(D_{jl}f_{kjl}^{(t)z} + \hat{f}_k^{(t)z}\right)\sin m\theta, \quad F_m^{(t)} = \sum_{k=0}^{K}\sum_{j=0}^{K}\sum_{l=1}^{4}D_{jl}f_{kjl}^{(t)m}\sin m\theta \tag{34c,d}$$

$$u_\rho^{(t)} = \sum_{k=0}^{K}\sum_{j=0}^{K}\sum_{l=1}^{4}\left(D_{jl}u_{kjl}^{(t)\rho} + \hat{u}_k^{(t)\rho}\right)\sin m\theta, \quad u_\theta^{(t)} = -\sum_{k=0}^{K}\sum_{j=0}^{K}\sum_{l=1}^{4}\left(D_{jl}u_{kjl}^{(t)\theta} + \hat{u}_k^{(t)\theta}\right)\cos m\theta \tag{35a,b}$$

$$u_z^{(t)} = \sum_{k=0}^{K}\sum_{j=0}^{K}\sum_{l=1}^{4}\left(D_{jl}u_{kjl}^{(t)z} + \hat{u}_k^{(t)z}\right)\sin m\theta, \quad \gamma_v^{(t)} = \sum_{k=0}^{K}\sum_{j=0}^{K}\sum_{l=1}^{4}\left(D_{jl}u_{kjl}^{(t)m} + \hat{u}_k^{(t)m}\right)\sin m\theta \tag{35c,d}$$

where the first items come from homogeneous solutions shown in Eq. (27) and the second, from particular solutions shown in Eqs. (24) and (25).

5. The continuity conditions at the intersecting curve

The above mentioned $(4K+2)$ unknowns C_{ni} in the general solutions for main shells and $(4K+4)$ unknowns D_{jl} in the general solutions for branch pipes are obtained from the continuity conditions at the intersecting curve, Γ, as follows:

$$F_\rho = -F_\rho^{(t)}, \quad F_\theta = -F_\theta^{(t)}, \quad F_z = -F_z^{(t)}, \quad M_v = M_v^{(t)} \tag{36a,b,c,d}$$

$$u_\rho = u_\rho^{(t)}, \quad u_\theta = u_\theta^{(t)}, \quad u_z = u_z^{(t)}, \quad \gamma_v = -\gamma_v^{(t)} \tag{37a,b,c,d}$$

Substituting Eqs. (22) and (23) into the left sides of Eqs. (36) and (37), and Eqs. (34) and (35) into the right sides, respectively, $(8K+8)$ continuity conditions for each harmonic of the Fourier series are given. However, some of the continuity conditions of the forces and moments, Eqs. ((36a)–(d)), are automatically satisfied due to the tee-joint in equilibrium in total, i.e., $F_x = F_y = F_z = M_y = M_z = 0$ and $M_x = M_{xb}$. Because the symmetry about $\theta = 0$ and the antisymmetry with respect to $\theta = \pi/2$ have been applied to the above mentioned Fourier series, only two equilibrant conditions remain as follows:

$$F_y = \oint_\Gamma [F_\rho \sin\theta - F_\theta \cos(\theta)]\, ds_\Gamma = 0 \tag{38a}$$

$$M_{xb} = \oint_\Gamma [RF_z\rho_0 \sin\theta - M_v \cos(\boldsymbol{i_t}, \boldsymbol{i_x})]\, ds_\Gamma \tag{38b}$$

Therefore, only two of the continuity conditions of general forces ((36a)–(d)) when $m = 1$ $(k = 0)$ are independent so that the first harmonic $(k = 0)$ of Eq. (36b,d) can be omitted. Then there are $(8K+6)$ independent equations for solving C_{ni} $(n = 1, 2 \ldots 2K+1;\ i = 1, 2)$ and D_{jl} $(j = 1, 2 \ldots K;\ l = 1, 2, 3, 4)$.

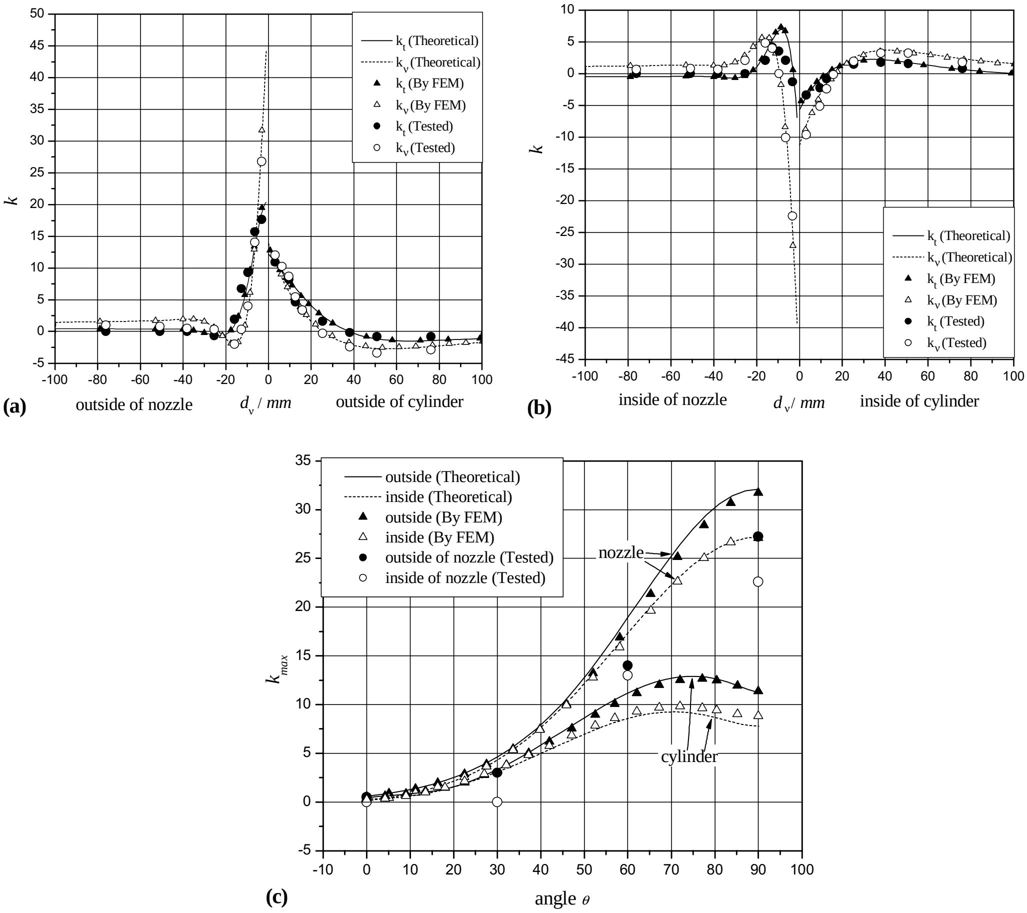

Fig. 4. (a) Distribution of k along the gauge line $\theta = 90°$ on the outer surface of Model ORNL-1; (b) distribution of k along the gauge line $\theta = 90°$ on the inner surface of Model ORNL-1; (c) variation of maximum principal stress ratios around the junction on the nozzle.

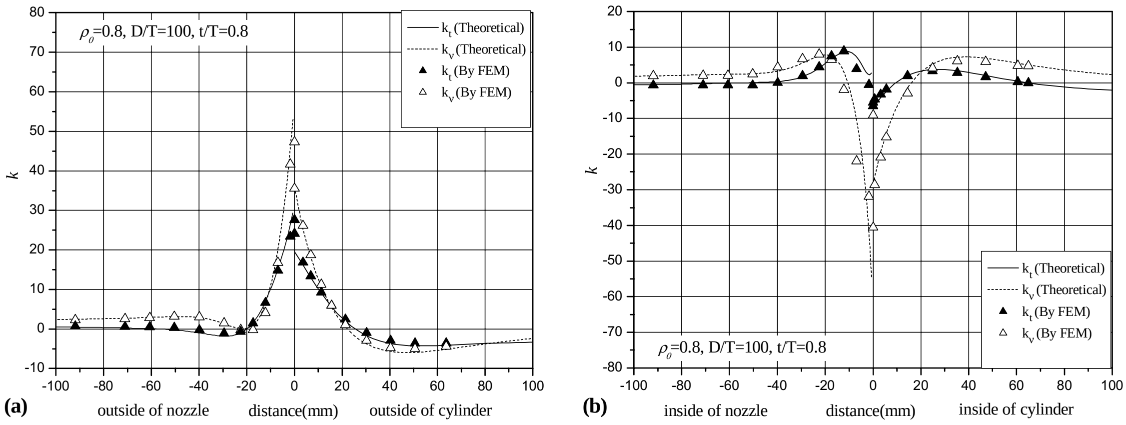

Fig. 5. Distribution of k along the line $\theta = 90°$ on the outer and inner surfaces of the model with parameters $d/D = 0.8$, $D/T = 100$, $t/T = 0.8$.

6. Verification of the present theoretical solution

6.1. Comparison with the test and the numerical results for model ORNL-1 ($d/D = t/T = 0.5$, $D/T = 100$)

The dimensionless normal stresses k_v and tangential stresses k_t obtained by the present theoretical solution, by test given by Corum et al. (1974) and by 3-D finite element method (the calculated FEM model by software ANSYS has 206,353 nodes and four layers of 20-nodal elements through the thickness in close vicinity to the intersection) are shown in Fig. 4(a,b,c); where, $k_v = \sigma_v/\sigma_0$, $k_t = \sigma_t/\sigma_0$, $k_{\max} = \sigma|_\Gamma/\sigma_0$ and $\sigma_0 = 4M_{xb}/\pi d^2 t$. Where, the subscript '$v$' and '$t$' are defined by Xue et al. (2000) and the same as Corum et al. (1974). The comparison shows that the results obtained by the three different methods are in very good agreement. Besides, Fig. 4(a,b,c) show that the stress concentration in nozzle is more significant than that in vessel when the branch pipe is relatively thinner than the main shell.

6.2. Comparison with the numerical results by 3-D FEM for a model with parameters $d/D = t/T = 0.8$, $D/T = 100$

A 3-D finite element model with parameters $d/D = t/T = 0.8$ and $D/T = 100$ ($\lambda = d/(DT)^{1/2} = 8$) is calculated by software ANSYS in order to verify the applicable range of parameters for the presented theoretical solution. The model has 41,450 20-nodal elements and 622,722 freedom degrees. The results obtained by the two methods are in good agreement as shown in Fig. 5(a) and (b).

7. Comparison of resultant forces and bending moments with WRC Bulletin 297

The methods shown in WRC Bulletin 297 based on analytical solution given by Steele and Steele (1983) are currently used in pressure vessel industry within the limits of $d/D \leqslant 0.5$ and $\lambda < 5$. Figs. 6 and 7 show that the results obtained by the presented method are in agreement with those given by WRC Bulletin 297 when d/D is small. In Fig. 6 M_r, M_θ, N_r and N_θ are the maximum values in the main shells.

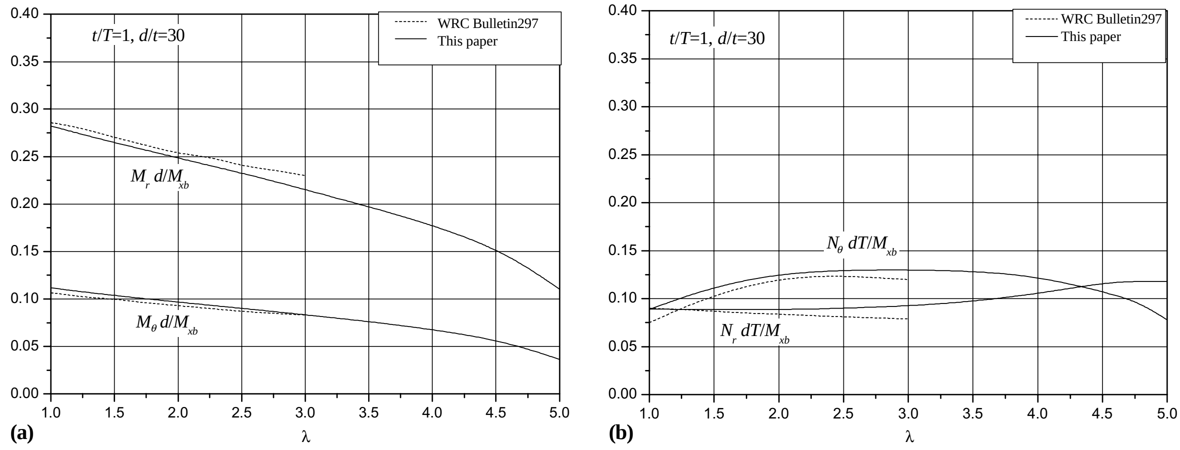

Fig. 6. The comparison of dimensionless resultant forces and moments at the junction of the main shell.

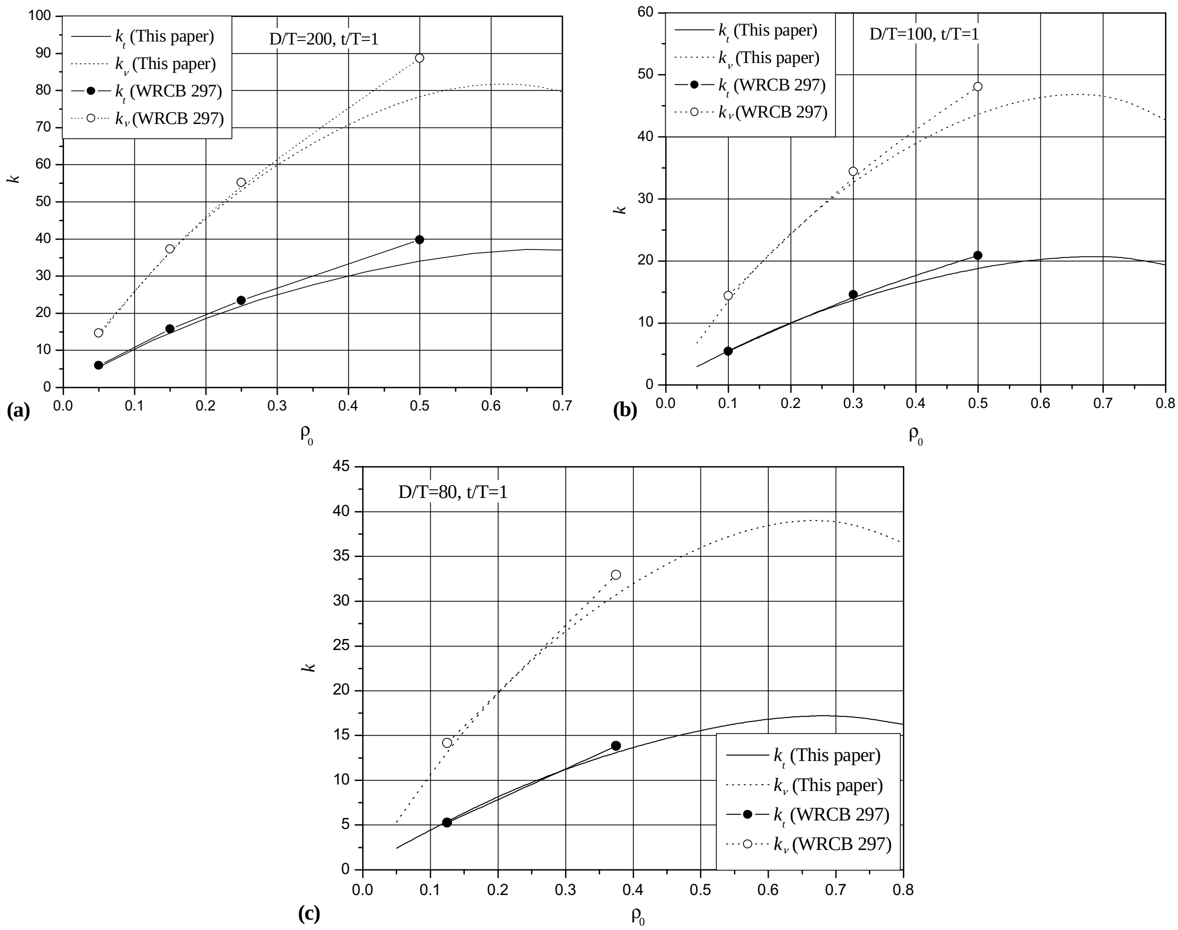

Fig. 7. The comparison of maximum dimensionless stresses at the junction of the main shell.

8. Conclusion

A thin shell theoretical solution of two normally intersecting cylindrical shells subjected to out-of plane branch pipe moment is presented. The results by the present method are in very good agreement with those obtained by test and by FEM. The analytical method can be applicable up to $d/D \leqslant 0.8$ and $\lambda = d/(DT)^{1/2} \leqslant 8$. The present analytical results are in good agreement with WRC Bulletin 297 when d/D is small.

References

Bijlaard, P.P., 1954. Stresses from radial loads in cylindrical pressure vessels. The Welding Journal 33 (12, Research Suppl.), 615-s–623-s.

Bijlaard, P.P., 1955a. Stresses from local loading in cylindrical pressure vessels. Trans. ASME 77, 805–812.

Bijlaard, P.P., 1955b. Stresses from radial loads and external moments in cylindrical pressure vessels. The Welding Journal 34 (12, Research Suppl.), 608s–617s.

Morley, L.S.D., 1959. An improvement on Donnell's approximation for thin-walled circular cylinders. Quart. J. Mech. Appl. Math. 12, 89.

Corum, J.M., Bolt, S.E., Greenstreet, W.L., Gawltney, R.C., 1974. Theoretical and experimental stress analysis of ORNL thin-shell cylinder to cylinder Model_1. ORNL Report 4553, Oak Ridge National Laboratory.

Davis, P.J., Rabinowitz, P., 1984. Methods of Numerical Integration, second ed. Academic Press, New York.

Deng, Y., Hwang, K.C., Xue, M.D., 1991. The stress analysis of cylindrical shells with rigid inclusions having a large ratio of radii. SMiRT 11 Transactions F, F05/2, (Tokyo) 85–90.

Eringen, A.C., Naghdi, A.K., Mahmood, S.S., Thiel, C.C., Ariman, T., 1969. Stress concentrations in two normally intersecting cylindrical shells subject to internal pressure. Welding Research Council Bulletin No. 139, April.

Eringen, A.C., Naghdi, A.K., Thiel, C.C., 1965. State of stress in a circular cylindrical shell with a circular hole. Welding Research Council Bulletin No. 102, January.

Eringen, A.C., Suhubi, E.S., 1965. Stress distribution at two normally intersecting cylindrical shells. Nucl. Struct. Eng. 2, 235–270.

Goldenveizer, A.L., 1961. Theory of Elastic Thin Shells. Pergamon Press, New York.

Hansberry, J.W., Jones, N., 1969. A Theoretical study of the elastic behavior of two normally intersecting cylindrical shells. J. Eng. Indus., 563–572.

Khathlan, A.A., 1986. Stresses at the junction of two normally intersecting circular cylinders. Ph.D. Thesis, Stanford University.

Lekerkerker, J.G.., 1972. The determination of elastic stresses near cylinder-to-cylinder intersection. Nucl. Eng. Des. 20, 57–84.

Mershon, J.L., Mokhtarian, K., Ranjan, G.V., Rodabaugh, E.C., 1984. Local stresses in cylindrical shells due to external loadings on nozzle sulement to WRC Bulletin No. 107. WRC Bulletin 297.

Moffat, D.G., 1985. Experimental stress analysis of four fabricated equal diameter branch pipe intersections subjected to moment loadings and the implications on branch junctions design. Proc. Inst. Mech. Engrs. 199, 261–284.

Moffat, D.G., Mwenifumbow, J.A.M., Xu, S.H., Mistry, J., 1991. Effective stress factors for piping branch junctions due to internal pressure and external moment loads. J. Strain Anal. 26 (2), 85–101.

Qian, L.X., Tang, X.J., Zhong, W.X., Yang, M.S., Chen, H.R., Shun, L.H., 1965. General solution of cylindrical shells with cut-out. J. Dalian Inst. Technol. 3 (4), 1–23 (in Chinese).

Reidelbach, W., 1961. The state of stress at the perpendicular intersection of two right circular tubes. Ingenieur Arch. 30 (5), 293–316 (in German).

Steele, C.R., Steele, M.L., 1983. Stress analysis of nozzle in cylindrical vessels with external load. ASME J. Pres. Ves. Tech. 105, 191–200.

Timoshenko, S., Woinowsky-Krieger, S., 1959. Theory of Plates and Shells, second ed. McGraw-Hill, New York. pp. 513–514.

Van Dyke, P., 1965. Stress about a circular hole in a cylindrical shell. AIAA J. 3 (9).

Van Dyke, P., 1967. Stress in a cylindrical shell with a rigid inclusion. AIAA J. 5 (1).

Wang, Z.X., Guo, D.R., 2000. Introduction to Special Functions. Peking University Press, Beijing. pp. 647–649 (in Chinese).

Wichman, K.R., Hopper, A.G., Mershon, J.L., 1965. Local stresses in spherical and cylindrical shells due to external loadings. WRC Bulletin No. 107.

Xue, M.D., Deng, Y., Hwang, K.C., 1991. Some results on analytical solution of cylindrical shells with large opening. ASME J. Pres. Ves. Tech. 113, 297–307.

Xue, M.D., Chen, W., Deng, Y., Hwang, K.C., 1995a. The thin shell theoretical solution for cylindrical shells with large openings. Acta Mech. Sinca 27 (4), 482–488 (in Chinese).

Xue, M.D., Chen, W., Hwang, K.C., 1995b. Stresses at the intersection of two cylindrical shells. Nucl. Eng. Des. 154, 231–238.

Xue, M.D., Hwang, K.C., Lü, W., Chen, W., 1996. A reinforcement design method based on analysis of large openings in cylindrical pressure vessels. ASME J. Pres. Ves. Tech. 118, 502–506.

Xue, M.D., Wang, H.H., Chen, W., Hwang, K.C., 1999. Analytical solution for cylindrical thin shells with normally intersecting nozzles due to external moments on the ends of shells. Sci. China A 42 (3), 293–304.

Xue, M.D., Wang, H.H., Hwang, K.C., 2000. Stress analysis of cylindrical shells with nozzles due to external run pipe moments. J. Strain Anal. Eng. Des. 35, 159–170.

Yamamoto, Y., Isshiki, H., Hayashi, T., Ukaji, H., 1969. Theory of stress concentration of two normally intersecting cylindrical shells. Bull. Jpn. Soc. Mech. Eng. 12 (49), 1–9.

Zhang, P.X., Hwang, K.C., Lu, M.W., 1991. Stress analysis of the cylindrical shell with a large opening. Acta Mech. Sinca 23 (6), 700–705 (in Chinese).